Title:

Reducing L-lactate release from hippocampal astrocytes by intracellular oxidation increases novelty induced activity in mice

Running title: Astrocytic lactate and novelty behaviour

Barbara Vaccari Cardoso[1]; Alexey V. Shevelkin[2]; Chantelle Terrillion[2]; Olga Mychko[2]; Valentina Mosienko[3]; Sergey Kasparov[1]; Mikhail V. Pletnikov[2,4^]; and Anja G. Teschemacher[1]

[1]School of Physiology, Pharmacology and Neuroscience, University of Bristol, Bristol, BS8 1TD, UK

[2]Department of Psychiatry and Behavioral Sciences, Johns Hopkins University School of Medicine, Baltimore, MD 21287, USA

[3]Institute of Biomedical and Clinical Sciences, College of Medicine and Health, University of Exeter, Exeter, EX4 4PS, UK

[4]Solomon H. Snyder Department of Neuroscience, Johns Hopkins University School of Medicine, Baltimore, MD 21205, USA

[^]Present address: Department of Physiology and Biophysics, University at Buffalo, NY 14203, USA

Acknowledgments: This work was supported by Science without Borders - CNPq (206427/2014-0 to BVC), BHF (PG/18/8/33540 to AGT), Northcott Devon Medical Trust Foundation Grant (TB/MG/NO5002 to VM); NIH (MH-083728, DA-041208, MH-094268 to MVP). The work at the JHU Neuroscience Multiphoton Imaging Core was supported by the NINDS grant (NS050274).

The authors declare no conflict of interest**.**

Total Word Count: 6874 words

Abstract (*178 words*)

Astrocytes are in control of metabolic homeostasis in the brain and support and modulate neuronal function in various ways. Astrocyte-derived L-lactate (LL) is thought to play a dual role as a metabolic and a signaling molecule in inter-cellular communication. The biological significance of LL release from astrocytes is poorly understood, largely because the tools to manipulate LL levels *in vivo* are limited. We therefore developed new viral vectors for astrocyte-specific expression of a mammalianised version of lactate oxidase (LOX) from *Aerococcus viridans*. LOX expression in astrocytes *in vitro* reduced their intracellular LL levels as well as the release of LL to the extracellular space. Selective expression of LOX in astrocytes of the dorsal hippocampus in mice resulted in increased locomotor activity in response to novel stimuli. Our findings suggest that a localised decreased intracellular LL pool in hippocampal astrocytes could contribute to greater responsiveness to environmental novelty. We expect that use of this molecular tool to chronically limit astrocytic LL release will significantly facilitate future studies into the roles and mechanisms of intercellular LL communication in the brain.

Keywords:

Astrocytes

L-lactate

Lactate oxidase

Lentiviral vector

Hippocampus

Behavior

Novelty

MAIN POINTS:

Lactate oxidase (LOX) expression limits the intra-astrocytic pool of lactate and decreases its release.

LOX in astrocytes of the dorsal mouse hippocampus causes increased activity in novel environment.

Introduction (*420 words*)

Astrocytes are the major regulators of brain metabolic homeostasis as they are able to import from the periphery, metabolize, store and dynamically shuttle energy substrates throughout the astrocytic network and into the brain's extracellular space (Marina et al., 2020; Verkhratsky et al., 2015; Weber & Barros, 2015). At the same time, astrocytes, by responding to local neuronal activity and the extracellular environment, actively participate in synaptic transmission and inter-cellular communication (Gourine et al., 2010; Halassa et al., 2007; Lalo et al., 2014; Mastitskaya et al., 2020). Astrocyte-derived L-lactate (LL), in particular, has gained increasing attention due to its dual role as a metabolic and signaling molecule in the brain (Barros & Weber, 2018; Karagiannis et al., 2015; Magistretti & Allaman, 2018; Marina et al., 2018, 2020; Mosienko et al., 2015, 2018).

During periods of increased local brain activity, astrocytes elevate their release of LL to support a wide range of brain area-dependent functions. Examples include promotion of learning and memory in hippocampus and cortex (Alberini et al., 2018; Newman et al., 2011; Yang et al., 2014; Zuend et al., 2020), cerebral angiogenesis (Morland et al., 2017), regulation of sympatho-excitation in the ventro-lateral medulla (Marina et al., 2015), improvement of decision making behavior by synchronisation of amygdala with anterior cingulate cortex (Wang et al., 2017), and amplification of the arousal response evoked by the *locus coeruleus* (Barros & Weber, 2018; Mosienko et al., 2018; Tang et al., 2014). LL is also known to modulate mood by as yet unknown mechanisms of action. Acute or chronic peripheral administration of LL in animal models of depression resulted in an antidepressant-like effect (Carrard et al., 2018; Jouroukhin et al., 2018; Karnib et al., 2019). This response was accompanied by increased levels of LL in the hippocampus as well as changes in the expression of genes associated with serotonin receptor trafficking, the astrocytic calcium-binding protein S100β, neurogenesis and cAMP signalling (Carrard et al., 2018).

However, the mechanisms whereby LL influences metabolic and signalling pathways are poorly understood as the tools to manipulate LL levels *in vivo* in a cell type-specific manner are limited. With this in mind, we developed a novel viral vector system to express a mammalianized version of lactate oxidase (LOX) from *Aerococcus viridans* under control of an enhanced astrocyte-specific promoter (Liu et al., 2008). Expression of LOX in primary astrocytes reduced their intracellular LL pool and limited the release of LL. In comparison to control mice, mice selectively expressing LOX in astrocytes of the hippocampus demonstrated increased responsiveness to novel environmental stimuli.

Materials and Methods (*1762 words*)

Viral vector construction

The sequence of Lactate oxidase (LOX; E.C. 1.1.3.15) from *Aerococcus viridans* (GenBank: D50611.1) was optimised for mammalian codon usage and synthesised by Invitrogen (Thermo Fisher Scientific UK).

For functional testing in HEK293 cells, we constructed pCMV-LOX-IRES-EGFP, an expression vector with CMV promoter where the LOX open reading frame was inserted in 5'-position of an internal ribosomal entry site (IRES), followed by green fluorescent protein (EGFP; Suppl Figure 1a). The equivalent cassette devoid of LOX served as control plasmid (pCMV-IRES-EGFP). Cells were transfected with TransIT-293 (Mirus, MIR 2700) 2-3 days prior to experiments.

For *in vitro* tests in primary astrocytes, an adenoviral vector (AVV), AVV-sGFAP-LOX-IRES-tdTomato (Suppl Figure 1b), was constructed by standard homologous recombination (Bett et al., 1994; Duale et al., 2005). In order to limit expression to astrocytes, we employed a transcriptionally enhanced shortened human GFAP promoter (sGFAP) (Liu et al., 2008). TdTomato was adopted as a reporter gene to avoid interference with the emission spectra of concomitantly used FRET sensor. Where indicated, AVV-sGFAP-EGFP was used as control.

For gene delivery into astrocytes *in vivo*, the expression cassette was transferred from AVV to a lentiviral vector (LVV), LVV-sGFAP-LOX-IRES-tdTomato (Suppl Figure 1c)

(Coleman et al., 2003; Duale et al., 2005; Teschemacher et al., 2005). LVV-sGFAP-IRES-tdTomato was created as a control vector.

Primary cultures

Neonate Wistar rats were used in accordance with Schedule 1 of the UK Home Office (Scientific Procedures) Act (1986) and as approved by the University of Bristol ethics committees. Primary astrocytes were cultured following protocols adapted from (Marriott et al., 1995). Brains were dissected from Wistar P2 pups, and the coronal section including midbrain and brainstem was dissociated by trituration following incubation in Hank's Balanced Salt Solution (HBSS) with DNase I (0.04 mg/mL), BSA (3 mg/mL), and bovine pancreas trypsin (0.25 mg/mL). Cells were incubated (37°C; 5% CO_2) in culture media (Dulbecco's Modified Eagle Medium, 10% heat-inactivated foetal bovine serum, 100 U/mL penicillin, 0.1 mg/mL streptomycin) for 7 days. Flasks were gently shaken overnight to eliminate microglia and oligodendrocytes and astrocytes were passaged. Following another 7 days in culture, AVVs were added to culture media 2-3 days prior to experiments to allow for optimal transgene expression.

Preparation of organotypic slice cultures followed the previously described protocol (Teschemacher et al., 2005). The brainstem was isolated from P7-8 Wistar pups and transferred to sterile dissection medium containing HBSS, 20 mM glucose, 10 mM MgCl2, 1 mM HEPES, 1 mM kynurenic acid, 0.5% phenol red, 100 U/mL penicillin and 0.1 mg/mL streptomycin (4°C). A vibrating microtome (7000 SMZ, Campden Instruments, Loughborough, UK) was used to cut 200µm-thick coronal slices. Slices were deposited on culture membranes (Millicell-CM, Millipore) in a six-well plates with media consisting of 49% Opti-MEM with GlutaMAX (Life Technologies, 51985026), 25% HBSS, 25% foetal bovine serum, 1% penicillin (10,000 units)/streptavidin(10 mL/L), 25mM glucose. Slices were transduced with ~10^9 TU/mL of AVV-sGFAP-LOX-IRES-tdTomato for expression of LOX specifically in astrocytes and kept at 37ºC and 5% CO_2 for 8-12 days prior to experimentation.

Cell viability assays

Primary astrocytes were exposed to a range of AVV-sGFAP-LOX-IRES-tdTomato titres, in order to determine the optimal multiplicity of infection (MOI) and avoid non-specific toxicity arising from overexpression in astrocytes. For the Trypan Blue exclusion assay, astrocytes were harvested by trypsinization and stained with trypan blue solution 0.4% (Sigma, T8154). The percentage of blue non-viable cells was determined. The XTT cell viability assay was performed according to the manufacturer's instructions (Cell Signalling Technology, 9095). The formazan absorbance after 2h, which is proportional to the number of metabolically viable cells, was read at 450 nm in a microplate reader (Tecan Infinite M200 PRO, Labtech).

Measurements of extracellular L-lactate *in vitro*

Constitutive release of LL into culture media was determined with a fluorometric assay (EnzyFluo L-Lactate Assay Kit, BioAssay Systems, EFLLC-100) following the manufacturer's instructions. Media were exchanged and subsequently sampled after 2h for HEK293 and 6h for astrocytes. Following the enzymatic reaction, fluorescence was determined in the microplate reader with 530nm excitation at 585nm emission. The LL concentrations were determined according to the LL standard curve.

Real-time measurement of LL release in organotypic slices was performed using amperometric LL biosensors (Sarissa Biomedical, UK, SBS-LAC-05-50, SBI-NUL-05-50). Sensors were calibrated by applying defined concentrations of LL to the chamber before and after each recording. Slices were transferred to the recording chamber and continuously superfused with HEPES-buffered solution (HBS; in mM: NaCl 137, KCl 5.4 or 3, Na_2HPO_4 0.34, KH_2PO_4 0.44, $CaCl_2$ 1.6, $MgSO_4$ 0.8, $NaHCO_3$ 4.2, HEPES 10, Glucose 5.5; pH 7.4) at 2.5 ml/min (32.5 ± 1ºC). The electrode potential was controlled by a potentiostat (Duo-Stat ME200+) and the signal was processed and analysed using a 1401 interface and Spike 2 software (Cambridge Electronic Design, UK). Electrodes were brought to contact with the slice surface and left to stabilise for at least 30 min. Sensors were then moved to a different area

of the slide and allowed to plateau following the initial contact, before measurements of the constitutive release (LL tone) were taken.

For forced LL efflux from the cells, a trans-acceleration protocol was employed by delivering 10mM pyruvate to the recording chamber (Mächler et al., 2016; San Martín et al., 2013; Zuend et al., 2020). This approach relies on the inward gradient of the monocarboxylate transporter (MCT) substrate pyruvate to trigger MCT-mediated LL extrusion from the cells (Fishbein et al., 1988).

Assessing intracellular L-lactate *in vitro*

Primary cultures of astrocytes on collagenised glass coverslips were transduced with an AVV to express the LL FRET sensor Laconic (San Martín et al., 2013) and co-transduced with AVV-sGFAP-LOX-IRES-tdTomato. Coverslips were transferred to a recording chamber mounted on an upright Leica confocal microscope (SP1 or SP5) and continuously superfused with HBS (glucose 2mM) at 2.5 ml/min (32.5 ± 1ºC). Laconic was excited with 458nm and emission bands for mTFP and Venus were sampled every 3 seconds for 465-500nm and 515-595nm bands, respectively. Regions of interest were analysed for the mTFP/Venus FRET ratio over time and average changes after pyruvate application were normalised to the baseline.

***In vivo* experiments**

Animals and Surgical procedures

C57Bl/6J mice (female, 8 weeks of age) were obtained from Jackson Lab and housed in groups of 3-5 animals in standard mouse cages on a 12-h light/dark cycle at a room temperature of 23°C with free access to food and water. The animal protocols were carried out in accordance with the Johns Hopkins University Animal Care and Use Committee. All experiments were performed during the light half of the cycle. Procedures were conducted using aseptic techniques. Mice were anesthetized with a 0.75% - 1% isoflurane-oxygen mixture (2% for induction) and placed in a supine position on a heating pad connected to a rectal thermometer (~37°C). For the dorsal hippocampus, 0.5 µL of LVV-sGFAP-IRES-

tdTomato (control; $5x10^9$ TU/mL) or LVV-sGFAP-LOX-IRES-tdTomato ($7x10^9$ TU/mL) were injected bilaterally into the dorsal CA1 area of the hippocampus (AP, ML, DV: -1.9 mm; ±1.4 mm; -1.6 mm) at 1 nL/sec using Nanoject III (Drummond Scientific Company, Broomall, PA), as previously described (Jouroukhin et al., 2019). After the injection, we waited 10 minutes before raising the glass micropipette. After surgery, mice were treated with buprenorphine (0.01 mg/kg s.c.) and Baytril (enrofloxacin, 2.5 mg/kg).

Behavioral tests

Mice were tested 4 weeks following surgery in a series of behavioural tests to assess novelty-induced activity in the open field, anxiety in the elevated plus maze (EPM), and exploratory activity in the hole board test. For the hole board test, the mice were placed in the center of a 40cm x 40cm hole board enclosure, with 16 three-centimeter holes spaced evenly (Stoelting Co., Illinois, USA). Mice were allowed to explore the hole board for 5 minutes. Distance travelled and head dips were recorded using Any-maze tracking software (Stoelting, Co.). These tests were followed by those for learning and memory: spontaneous alternation and spatial recognition in the Y maze, the novel object recognition test (NORT) and novel place recognition test (NPRT) and trace fear conditioning as previously described in (Abazyan et al., 2010, 2014; Pletnikov et al., 2008; Jouroukhin et al., 2018; Terrillion et al., 2017). All tests were conducted in the order that minimized potential carry-over effects and stressful experience confounds, namely, with a one-week interval between tests and from less to more stressful tests.

Immunohistochemistry

Transgene expression in primary cultured astrocytes and organotypic brainstem slices was confirmed by immunoreactivity to red fluorescent protein (RFP). Cells were fixed with ice-cold 4%paraformaldehyde (PFA) in 0.1 M phosphate buffer (PBS; pH 7.4), rinsed with PBS and incubated in a blocking and permeabilizing solution for 1 hour at room temperature (RT), followed by incubation with the anti-RFP primary antibody (1:200, Suppl Table 1) overnight at

4°C. An Alexa Fluor 594-labeled species-specific secondary antibody was used. Images were obtained with an upright Leica SP5 confocal laser-scanning microscope with 25x or 40x water immersion objective lenses.

Upon completion of behavioural tests, mice were deeply anesthetized with Forane (isoflurane USP, NDC 10019-360-60, Baxter Healthcare Corporation, Deerfield, IL, USA), followed by transcardial perfusion with ice-cold 0.1 M PBS and 4% PFA in 0.1 M PBS. The brains were dissected out and post-fixed in 4% PFA in 0.1 M PBS for 24h at 4ºC. After cryoprotection in 30% sucrose in 0.1 M PBS for 48 h, the brains were cut into 40 µm thick coronal sections.

The transduced brain areas were identified by their expression of tdTomato. To evaluate the brain cell types that were transduced with LVV, brain sections were stained with chicken anti-GFAP (1:1000), rabbit anti-S100 beta (1:1000), rabbit anti-Iba1 (1:1000) or Guinea pig anti-NeuN (1:1000) antibodies as previously described (Hoffman et al., 2016; Jouroukhin et al., 2019). Briefly, after incubating brain sections in the blocking solution for 1 h at RT, the sections were incubated for 48 hours at 4°C with the primary antibodies. Afterwards, the sections were incubated for 2 hours at RT with the corresponding Alexa 488-, 568-, 633-labeled species-specific secondary antibodies (1:1000) followed by three 5-min 3xPBS washes and DAPI 10 min staining (1:10000). Images were taken with a Zeiss 880 confocal laser-scanning microscope with 40x/1.3 oil DIC or 100x/1.46 oil DIC objectives at the Johns Hopkins University Neuroscience Multiphoton/Electrophysiology Core Facility.

Statistical Analysis

Data were subjected to a Shapiro–Wilk normality test. Groups were compared using paired or unpaired two-tails *t*-tests, ANOVA followed by Bonferroni's Multiple Comparison post hoc test, or non-parametric Wilcoxon-Mann–Whitney U test, as indicated. Box-and-whisker diagrams illustrate the upper and lower quartile values (boxes), median (central horizontal line), mean (central plus sign), and minimum and maximum data range (whiskers). Statistical

tests were performed using GraphPad Prism. Statistical difference of $p<0.05$ between the experimental groups was considered significant.

Results (642 *words*)

***In vitro* effects of LOX expression**

Astrocytes transduced with AVV-sGFAP-LOX-IRES-tdTomato at MOI 15 in dissociated primary cultures and with 10^9 TU/mL in organotypic slices displayed typical *in vitro* morphology and their survival was not compromised compared to un-transduced cultures (Suppl Figure 2b,c). A range of MOIs of AVV-sGFAP-LOX-IRES-tdTomato was used to transduce cultures, and their viability was assessed by Trypan Blue exclusion assay and XTT assay. In neither assay did control vector AVV-sGFAP-EGFP compromise the viability of astrocytes below an MOI of 50 (Figure 1). Therefore, all the functional validation experiments were carried out at MOI 15.

LOX expression reduces constitutive L-lactate release *in vitro*

The effect of LOX expression on release of LL was assessed in HEK293 cells and in primary astrocytes. Expression of a reporter fluorophore confirmed that the majority of cells were expressing the transgenes (Suppl Figure 2a,b). Concentration of LL in the conditioned extracellular media was significantly decreased by LOX (33.2% in HEK293 cells and 15.4% in astrocytes), reflecting limited constitutive LL release (Figure 2a,b). In line with this, amperometric recordings revealed that expression of LOX by astrocytes in organotypic slices significantly decreased LL tone when compared to control slices (Figure 2c).

LOX expression reduces the intracellular L-lactate pool *in vitro*

The change in intracellular LL was measured with confocal Laconic imaging while forcing LL depletion via pyruvate-evoked trans-acceleration (Mächler et al., 2016; San Martín et al., 2013; Zuend et al., 2020). As expected, bath application of pyruvate (10mM) evoked a substantial

drop in the intracellular concentration of LL in cultured dissociated astrocytes which was significantly decreased in LOX-expressing cultures (Figure 2d,e).

Trans-acceleration in cultured brainstem slices evoked an immediate and distinct peak in the extracellular concentration of LL in all slices (Figure 2f). The net amplitude of trans-acceleration-driven LL release was significantly reduced by 65.8% in slices transduced with AVV-sGFAP-LOX-IRES-tdTomato (Figure 2g). Pyruvate-driven LL release was followed by a transient decrease in LL concentration (depletion amplitude; Figure 2f) which is thought to reflect the depletion of the readily available intracellular LL pool that normally overflows as constitutive release. The drop from baseline LL to the following minimum LL release was reduced by 78.5% in slice cultures containing LOX-expressing astrocytes, suggesting, again, a diminished intra-astrocytic LL pool (Figure 2h).

In vivo effects of LOX expression in astrocytes of dorsal hippocampus

Analysis of expression of tdTomato indicated that LVV-sGFAP-LOX-IRES-tdTomato transduced astrocytes within a limited area of the dorsal hippocampus (Figure 3a). Using the anti-RFP antibody, we observed a wider spread of transgene expression (Figure 3b). Expression driven by this LVV was selective for astrocytes as no positive staining was seen in neurones or microglia (Suppl Figures 3-4).

Expression of LOX in hippocampal astrocytes did not alter general activity of mice in the open field test, including central, peripheral or rearing activities (Suppl Figure 5). No effects of LOX expression were observed on anxiety-like behaviour in the EPM (Suppl Figure 6). Compared to control mice, mice expressing LOX in astrocytes exhibited a significantly increased locomotor activity in the hole board test without altering number of head dips, suggesting elevated novelty-induced activity (Figure 3c, Suppl Figure 6). In addition, mice expressing LOX showed significantly less freezing behaviour during the habituation session in the trace fear conditioning test, indicative of elevated reactivity to unfamiliar environment (Figure 3d). When we assessed the effects of LOX on learning and memory, no significant changes were seen in spontaneous alterations in the Y maze test, the novel object recognition

test or the context- or cue-dependent conditional freezing in the trace fear conditioning test (Figure 3f,g; Suppl Figure 7). In contrast, compared to control mice, mice expressing LOX demonstrated a superior spatial recognition memory in the Y maze (Figure 3e). Collectively, our findings suggest that expression of LOX in hippocampal astrocytes led to increased responsiveness to novelty in mice that could facilitate some types of recognition memory.

Discussion (795 *words*)

The release of LL in the brain is not only dependent on its production rate but astrocytes have the ability to retain higher intracellular LL levels as a readily releasable pool which is available for stimulus-evoked transient release (Mächler et al., 2016; Sotelo-Hitschfeld et al., 2015). Here we report the validation and application of a novel viral vector-based molecular approach, designed to limit the intra-astrocytic LL pool without directly interfering with astrocytic LL production or release mechanisms (Figure 4). We have confirmed *in vitro* that LOX is enzymatically active and changes LL dynamics in dissociated cultured astrocytes and organotypic brainstem slices. Astrocyte-specific expression of LOX reduced the constitutive release of LL, as well as that evoked using a trans-acceleration protocol. Although trans-acceleration of MCTs has been recurrently used *in vitro* and *in vivo* to deplete cells of LL, this effect comes at the expense of cellular overload with pyruvate, which could result in LDH-mediated conversion of pyruvate to LL, increasing cytosolic LL concentration. In order to restrict LL formation following pyruvate application, the glucose concentration in the superfusion buffer was reduced so that the generation of NADH through glycolysis was limited and, with it, the activity of lactate dehydrogenase (San Martín et al., 2013). We found that trans-accelerated LL extrusion was substantially decreased in organotypic brainstem slices that contained both neurones and astrocytes. However, as LOX expression was targeted to astrocytes, our findings suggest that limiting the LL pool selectively in astrocytes makes a significant impact on LL dynamics in the integrated brain environment.

The degradation of LL to pyruvate by LOX results in production of hydrogen peroxide (Maeda-Yorita et al., 1995; Stoisser et al., 2016) (Figure 4). Whilst peroxide is a potentially

harmful molecule, astrocytes have been shown to exhibit a high glutathione content and a robust capacity for glutathione-dependent detoxification (Dringen et al., 2015; Liu et al., 2017). In order to minimize the potentially cytotoxic effects of ROS-mediated cellular damage or overexpression of a foreign protein product on astrocytic metabolism, we optimised vector titers to express LOX at the levels that did not seem to lead to any untoward consequences. Our *in vivo* observation do not suggest overt toxic effects on astrocytes either but future studies will perform a more detailed evaluation of possible ROS-mediated cellular effects of LOX expression.

The behavioural effects of astrocyte-restricted expression of LOX in the dorsal hippocampus suggest that decreased release of LL by hippocampal astrocytes increased responsiveness to novelty and did not affect anxiety in mice. These changes are consistent with the different functions of the dorsal vs. ventral hippocampus. It has been shown that the processing of novelty and spatial information is predominantly associated with the dorsal sub-regions of the hippocampus, while emotionality and anxiety have been preferentially attributed to the ventral areas of the hippocampus (Bannerman et al., 2014). This also concords with studies showing that peripheral LL administration did not alter baseline anxiety in rodents (Karnib et al., 2019).

Our behavioural results are consistent with numerous findings from humans, nonhuman primates, and rodents that the hippocampus plays the central role in the novelty detection, and the activity of the hippocampal circuits increases in response to novel stimuli (Murty et al., 2013). On the one hand, increased activity in the hole board test is in line with increased exploratory activity in LOX expressing animals. On the other hand, as LOX expression led to low freezing during the habituation stage in TFC, one could propose that decreased LL release by hippocampal astrocytes might affect habituation to the novel environment in mice. Notably, a recent study reports that selective chemogenetic activation of striatal astrocytes produced “acute behavioural hyperactivity and disrupted attention” and that thrombospodin-1 in astrocytes was required for manifestation of the behavioural phenomena (Nagai et al., 2019). It is tempting to speculate that our findings point to another possible

pathway that could be at play in the neuron-astrocyte interactions underlying the higher functions of the hippocampus. Further, one could hypothesize that given the short period of time during which the mice were behaviourally evaluated, our data suggest a signalling rather than metabolic role for LL in the tests used. Future studies using viral vector mediated LOX expression will help shed more light on the mechanisms and processes whereby astrocyte LL is involved in inter-cellular communications in the brain.

In conclusion, astrocyte-specific expression of LOX to limit intracellular LL pools represents a novel approach to elucidate the functions of LL in different brain cells. This approach allows for manipulating LL dynamics in chronic studies to elucidate the roles of LL in intercellular signalling and/or energy metabolism. We anticipate that the present study will facilitate a more accurate and nuanced understanding of how astrocytic LL contributes to the central networks in various physiological and pathological contexts (Figure 4).

References

Abazyan, B., Dziedzic, J., Hua, K., Abazyan, S., Yang, C., Mori, S., Pletnikov, M. V., & Guilarte, T. R. (2014). Chronic Exposure of Mutant DISC1 Mice to Lead Produces Sex-Dependent Abnormalities Consistent With Schizophrenia and Related Mental Disorders: A Gene-Environment Interaction Study. *Schizophrenia Bulletin*, *40*(3), 575–584. https://doi.org/10.1093/schbul/sbt071

Abazyan, B., Nomura, J., Kannan, G., Ishizuka, K., Tamashiro, K. L., Nucifora, F., Pogorelov, V., Ladenheim, B., Yang, C., Krasnova, I. N., Cadet, J. L., Pardo, C., Mori, S., Kamiya, A., Vogel, M. W., Sawa, A., Ross, C. A., & Pletnikov, M. V. (2010). Prenatal Interaction of Mutant DISC1 and Immune Activation Produces Adult Psychopathology. *Biological Psychiatry*, *68*(12), 1172–1181. https://doi.org/10.1016/j.biopsych.2010.09.022

Alberini, C. M., Cruz, E., Descalzi, G., Bessières, B., & Gao, V. (2018). Astrocyte glycogen and lactate: New insights into learning and memory mechanisms. *Glia*, *66*(6), 1244–1262. https://doi.org/10.1002/glia.23250

Bannerman, D. M., Sprengel, R., Sanderson, D. J., McHugh, S. B., Rawlins, J. N. P., Monyer, H., & Seeburg, P. H. (2014). Hippocampal synaptic plasticity, spatial memory and anxiety. *Nature Reviews Neuroscience*, *15*(3), 181–192. https://doi.org/10.1038/nrn3677

Barros, L. F., & Weber, B. (2018). CrossTalk proposal: an important astrocyte-to-neuron lactate shuttle couples neuronal activity to glucose utilisation in the brain. *The Journal of Physiology*, *596*(3), 347–350. https://doi.org/10.1113/JP274944

Bett, A. J., Haddara, W., Prevec, L., & Graham, F. L. (1994). An efficient and flexible system for construction of adenovirus vectors with insertions or deletions in early regions 1 and 3. *Proceedings of the National Academy of Sciences of the United States of America*, *91*(19), 8802–8806. https://doi.org/10.1073/pnas.91.19.8802

Carrard, A., Elsayed, M., Margineanu, M., Boury-Jamot, B., Fragnière, L., Meylan, E. M., Petit, J. M., Fiumelli, H., Magistretti, P. J., & Martin, J. L. (2018). Peripheral administration of lactate produces antidepressant-like effects. *Molecular Psychiatry*, *23*(2), 392–399. https://doi.org/10.1038/mp.2016.179

Coleman, J. E., Huentelman, M. J., Kasparov, S., Metcalfe, B. L., Paton, J. F. R., Katovich, M. J., Semple-Rowland, S. L., & Raizada, M. K. (2003). Efficient large-scale production and concentration of HIV-1-based lentiviral vectors for use in vivo. *Physiological Genomics*, *12*(3), 221–228. https://doi.org/10.1152/physiolgenomics.00135.2002

Dringen, R., Brandmann, M., Hohnholt, M. C., & Blumrich, E. M. (2015). Glutathione-Dependent Detoxification Processes in Astrocytes. *Neurochemical Research*, *40*(12), 2570–2582. https://doi.org/10.1007/s11064-014-1481-1

Duale, H., Kasparov, S., Paton, J. F. R., & Teschemacher, A. G. (2005). Differences in transductional tropism of adenoviral and lentiviral vectors in the rat brainstem. *Experimental Physiology*, *90*(1), 71–78. https://doi.org/10.1113/expphysiol.2004.029173

Fishbein, W. N., Foellmer, J. W., Davis, J. I., Fishbein, T. M., & Armbrustmacher, P. (1988). Clinical assay of the human erythrocyte lactate transporter. *Biochemical Medicine and Metabolic Biology*, *39*(3), 338–350. https://doi.org/10.1016/0885-4505(88)90094-1

Gourine, A. V, Kasymov, V., Marina, N., Tang, F., Figueiredo, M. F., Lane, S., Teschemacher, A. G., Spyer, K. M., Deisseroth, K., & Kasparov, S. (2010). Astrocytes Control Breathing Through pH-Dependent Release of ATP. *Science*, *329*(5991), 571–575. https://doi.org/10.1126/science.1190721

Halassa, M. M., Fellin, T., & Haydon, P. G. (2007). The tripartite synapse: roles for gliotransmission in health and disease. *Trends in Molecular Medicine*, *13*(2), 54–63. https://doi.org/10.1016/j.molmed.2006.12.005

Hoffman, G. E., Murphy, K. J., & Sita, L. V. (2016). The Importance of Titrating Antibodies for Immunocytochemical Methods. *Current Protocols in Neuroscience*, *76*(1), 2.12.1-2.12.37.

https://doi.org/10.1002/cpns.1

Jouroukhin, Y., Kageyama, Y., Misheneva, V., Shevelkin, A., Andrabi, S., Prandovszky, E., Yolken, R. H., Dawson, V. L., Dawson, T. M., Aja, S., Sesaki, H., & Pletnikov, M. V. (2018). DISC1 regulates lactate metabolism in astrocytes: implications for psychiatric disorders. *Translational Psychiatry*, *8*(1), 76. https://doi.org/10.1038/s41398-018-0123-9

Jouroukhin, Y., Zhu, X., Shevelkin, A. V., Hasegawa, Y., Abazyan, B., Saito, A., Pevsner, J., Kamiya, A., & Pletnikov, M. V. (2019). Adolescent Δ9-Tetrahydrocannabinol Exposure and Astrocyte-Specific Genetic Vulnerability Converge on Nuclear Factor-κB–Cyclooxygenase-2 Signaling to Impair Memory in Adulthood. *Biological Psychiatry*, *85*(11), 891–903. https://doi.org/10.1016/j.biopsych.2018.07.024

Karagiannis, A., Sylantyev, S., Hadjihambi, A., Hosford, P. S., Kasparov, S., & Gourine, A. V. (2015). Hemichannel-mediated release of lactate. *Journal of Cerebral Blood Flow & Metabolism*, *36*(7), 1202–1211. https://doi.org/10.1177/0271678X15611912

Karnib, N., El-Ghandour, R., El Hayek, L., Nasrallah, P., Khalifeh, M., Barmo, N., Jabre, V., Ibrahim, P., Bilen, M., Stephan, J. S., Holson, E. B., Ratan, R. R., & Sleiman, S. F. (2019). Lactate is an antidepressant that mediates resilience to stress by modulating the hippocampal levels and activity of histone deacetylases. *Neuropsychopharmacology*, *44*(6), 1152–1162. https://doi.org/10.1038/s41386-019-0313-z

Lalo, U., Palygin, O., Rasooli-Nejad, S., Andrew, J., Haydon, P. G., & Pankratov, Y. (2014). Exocytosis of ATP From Astrocytes Modulates Phasic and Tonic Inhibition in the Neocortex. *PLoS Biology*, *12*(1). https://doi.org/10.1371/journal.pbio.1001747

Liu, B., Paton, J. F., & Kasparov, S. (2008). Viral vectors based on bidirectional cell-specific mammalian promoters and transcriptional amplification strategy for use in vitro and in vivo. *BMC Biotechnology*, *8*, 49. https://doi.org/10.1186/1472-6750-8-49

Liu, B., Teschemacher, A. G., & Kasparov, S. (2017). Neuroprotective potential of astroglia. *Journal of Neuroscience Research*, *95*(11), 2126–2139. https://doi.org/10.1002/jnr.24140

Mächler, P., Wyss, M. T., Elsayed, M., Stobart, J., Gutierrez, R., von Faber-Castell, A., Kaelin, V., Zuend, M., San Martín, A., Romero-Gómez, I., Baeza-Lehnert, F., Lengacher, S., Schneider, B. L., Aebischer, P., Magistretti, P. J., Barros, L. F., & Weber, B. (2016). In Vivo Evidence for a Lactate Gradient from Astrocytes to Neurons. *Cell Metabolism*, *23*(1), 94–102. https://doi.org/10.1016/j.cmet.2015.10.010

Maeda-Yorita, K., Aki, K., Sagai, H., Misaki, H., & Massey, V. (1995). L-lactate oxidase and L-lactate monooxygenase: Mechanistic variations on a common structural theme. *Biochimie*,

77(7–8), 631–642. https://doi.org/10.1016/0300-9084(96)88178-8

Magistretti, P. J., & Allaman, I. (2018). Lactate in the brain: from metabolic end-product to signalling molecule. *Nature Reviews Neuroscience*, *19*(4), 235–249. https://doi.org/10.1038/nrn.2018.19

Marina, N., Ang, R., Machhada, A., Kasymov, V., Karagiannis, A., Hosford, P. S., Mosienko, V., Teschemacher, A. G., Vihko, P., Paton, J. F. R., Kasparov, S., & Gourine, A. V. (2015). Brainstem hypoxia contributes to the development of hypertension in the spontaneously hypertensive rat. *Hypertension*, *65*(4), 775–783. https://doi.org/10.1161/HYPERTENSIONAHA.114.04683

Marina, N., Christie, I. N., Korsak, A., Doronin, M., Brazhe, A., Hosford, P. S., Wells, J. A., Sheikhbahaei, S., Humoud, I., Paton, J. F. R., Lythgoe, M. F., Semyanov, A., Kasparov, S., & Gourine, A. V. (2020). Astrocytes monitor cerebral perfusion and control systemic circulation to maintain brain blood flow. *Nature Communications*, *11*(1), 131. https://doi.org/10.1038/s41467-019-13956-y

Marina, N., Turovsky, E., Christie, I. N., Hosford, P. S., Hadjihambi, A., Korsak, A., Ang, R., Mastitskaya, S., Sheikhbahaei, S., Theparambil, S. M., & Gourine, A. V. (2018). Brain metabolic sensing and metabolic signaling at the level of an astrocyte. *Glia*, *66*(6), 1185–1199. https://doi.org/10.1002/glia.23283

Marriott, D. R., Hirst, W. D., & Ljungberg, M. C. (1995). Astrocytes. In J. Cohen & G. P. Wilkin (Eds.), *Neural cell culture - A practical approach* (pp. 85–96). Oxford University Press.

Mastitskaya, S., Turovsky, E., Marina, N., Theparambil, S. M., Hadjihambi, A., Kasparov, S., Teschemacher, A. G., Ramage, A. G., Gourine, A. V., & Hosford, P. S. (2020). Astrocytes Modulate Baroreflex Sensitivity at the Level of the Nucleus of the Solitary Tract. *The Journal of Neuroscience*, *40*(15), 3052–3062. https://doi.org/10.1523/JNEUROSCI.1438-19.2020

Morland, C., Andersson, K. A., Haugen, Ø. P., Hadzic, A., Kleppa, L., Gille, A., Rinholm, J. E., Palibrk, V., Diget, E. H., Kennedy, L. H., Stølen, T., Hennestad, E., Moldestad, O., Cai, Y., Puchades, M., Offermanns, S., Vervaeke, K., Bjørås, M., Wisløff, U., Storm-Mathisen, J., & Bergersen, L. H. (2017). Exercise induces cerebral VEGF and angiogenesis via the lactate receptor HCAR1. *Nature Communications*, *8*(7491), 15557. https://doi.org/10.1038/ncomms15557

Mosienko, V., Rasooli-Nejad, S., Kishi, K., De Both, M., Jane, D., Huentelman, M., Kasparov, S., & Teschemacher, A. (2018). Putative Receptors Underpinning l-Lactate Signalling in Locus Coeruleus. *Neuroglia*, *1*(2), 365–380. https://doi.org/10.3390/neuroglia1020025

Mosienko, V., Teschemacher, A. G., & Kasparov, S. (2015). Is L-Lactate a Novel Signaling Molecule in the Brain? *Journal of Cerebral Blood Flow & Metabolism*, *35*(7), 1069–1075. https://doi.org/10.1038/jcbfm.2015.77

Murty, V. P., Ballard, I. C., Macduffie, K. E., Krebs, R. M., & Adcock, R. A. (2013). Hippocampal networks habituate as novelty accumulates. *Learning & Memory*, *20*(4), 229–235. https://doi.org/10.1101/lm.029728.112

Nagai, J., Rajbhandari, A. K., Gangwani, M. R., Hachisuka, A., Coppola, G., Masmanidis, S. C., Fanselow, M. S., & Khakh, B. S. (2019). Hyperactivity with Disrupted Attention by Activation of an Astrocyte Synaptogenic Cue. *Cell*, *177*(5), 1280-1292.e20. https://doi.org/10.1016/j.cell.2019.03.019

Newman, L. A., Korol, D. L., & Gold, P. E. (2011). Lactate Produced by Glycogenolysis in Astrocytes Regulates Memory Processing. *PLoS ONE*, *6*(12), e28427. https://doi.org/10.1371/journal.pone.0028427

Pletnikov, M. V, Ayhan, Y., Nikolskaia, O., Xu, Y., Ovanesov, M. V, Huang, H., Mori, S., Moran, T. H., & Ross, C. A. (2008). Inducible expression of mutant human DISC1 in mice is associated with brain and behavioral abnormalities reminiscent of schizophrenia. *Molecular Psychiatry*, *13*(2), 173–186. https://doi.org/10.1038/sj.mp.4002079

San Martín, A., Ceballo, S., Ruminot, I., Lerchundi, R., Frommer, W. B., & Barros, L. F. (2013). A Genetically Encoded FRET Lactate Sensor and Its Use To Detect the Warburg Effect in Single Cancer Cells. *PLoS ONE*, *8*(2), e57712. https://doi.org/10.1371/journal.pone.0057712

Sotelo-Hitschfeld, T., Niemeyer, M. I., Machler, P., Ruminot, I., Lerchundi, R., Wyss, M. T., Stobart, J., Fernandez-Moncada, I., Valdebenito, R., Garrido-Gerter, P., Contreras-Baeza, Y., Schneider, B. L., Aebischer, P., Lengacher, S., San Martin, A., Le Douce, J., Bonvento, G., Magistretti, P. J., Sepulveda, F. V., Weber, B., & Barros, L. F. (2015). Channel-Mediated Lactate Release by K+-Stimulated Astrocytes. *Journal of Neuroscience*, *35*(10), 4168–4178. https://doi.org/10.1523/JNEUROSCI.5036-14.2015

Stoisser, T., Brunsteiner, M., Wilson, D. K., & Nidetzky, B. (2016). Conformational flexibility related to enzyme activity: evidence for a dynamic active-site gatekeeper function of Tyr215 in Aerococcus viridans lactate oxidase. *Scientific Reports*, *6*(1), 27892. https://doi.org/10.1038/srep27892

Tang, F., Lane, S., Korsak, A., Paton, J. F. R., Gourine, A. V, Kasparov, S., & Teschemacher, A. G. (2014). Lactate-mediated glia-neuronal signalling in the mammalian brain. *Nature Communications*, *5*, 3284. https://doi.org/10.1038/ncomms4284

Terrillion, C. E., Abazyan, B., Yang, Z., Crawford, J., Shevelkin, A. V, Jouroukhin, Y., Yoo, K. H., Cho, C. H., Roychaudhuri, R., Snyder, S. H., Jang, M.-H., & Pletnikov, M. V. (2017). DISC1 in Astrocytes Influences Adult Neurogenesis and Hippocampus-Dependent Behaviors in Mice. *Neuropsychopharmacology*, *42*(11), 2242–2251. https://doi.org/10.1038/npp.2017.129

Teschemacher, A. G., Paton, J. F. R., & Kasparov, S. (2005). Imaging living central neurones using viral gene transfer. *Advanced Drug Delivery Reviews*, *57*(1), 79–93. https://doi.org/10.1016/j.addr.2004.05.004

Verkhratsky, A., Nedergaard, M., & Hertz, L. (2015). Why are Astrocytes Important? *Neurochemical Research*, *40*(2), 389–401. https://doi.org/10.1007/s11064-014-1403-2

Wang, J., Tu, J., Cao, B., Mu, L., Yang, X., Cong, M., Ramkrishnan, A. S., Chan, R. H. M., Wang, L., & Li, Y. (2017). Astrocytic L-Lactate Signaling Facilitates Amygdala-Anterior Cingulate Cortex Synchrony and Decision Making in Rats. *Cell Reports*, *21*(9), 2407–2418. https://doi.org/10.1016/j.celrep.2017.11.012

Weber, B., & Barros, L. F. (2015). The Astrocyte: Powerhouse and Recycling Center. *Cold Spring Harbor Perspectives in Biology*, *7*(12), a020396. https://doi.org/10.1101/cshperspect.a020396

Yang, J., Ruchti, E., Petit, J.-M., Jourdain, P., Grenningloh, G., Allaman, I., & Magistretti, P. J. (2014). Lactate promotes plasticity gene expression by potentiating NMDA signaling in neurons. *Proceedings of the National Academy of Sciences*, *111*(33), 12228–12233. https://doi.org/10.1073/pnas.1322912111

Zuend, M., Saab, A. S., Wyss, M. T., Ferrari, K. D., Hösli, L., Looser, Z. J., Stobart, J. L., Duran, J., Guinovart, J. J., Barros, L. F., & Weber, B. (2020). Arousal-induced cortical activity triggers lactate release from astrocytes. *Nature Metabolism*, *2*(2), 179–191. https://doi.org/10.1038/s42255-020-0170-4

Data Availability Statement: Data available on request from the authors

Figure Legends

Figure 1. *In vitro* viability of AVV-transduced cultured astrocytes expressing LOX or a control reporter. Trypan Blue exclusion assay **(a)** and XTT assay **(b)** consistently reported no effect of AVV-sGFAP-LOX-IRES-tdTomato on cell viability below an AVV MOI of 50; cell viability was unaffected by transduction with reporter (EGFP) expressing control AVV across the range of tested MOI ratios. **(a)** Sample sizes n=8 wells in No AVV, n=5 and n=6 wells in Control MOI 15 and 50, respectively, and n=6 and n=5 wells in LOX MOI 15 and MOI 50, respectively. **(b)** Sample sizes n=6 wells in no AVV, and n=9 wells in Control and LOX at all MOIs tested. ANOVA (Bonferroni's Multiple Comparison Test) for comparison between control AVV transduction and un-transduced astrocytes; unpaired two-tailed t-test for comparison of LOX to control reporter expressing astrocytes at each MOI tested.

Figure 2. LOX expression reduces LL release *in vitro*. (a) Media conditioned for 2 hours by HEK293 cells transfected with 1µg/µl of either pCMV-IRES-EGFP (Control, n=6 wells) or pCMV-LOX-IRES-EGFP (LOX, n=9 wells; unpaired two-tailed t-test). **(b)** Media conditioned for 6 hours by dissociated cultured astrocytes transduced with AVV-sGFAP-EGFP (Control, n=18 wells) or AVV-sGFAP-LOX-IRES-tdTomato (LOX, n=9 wells; unpaired two-tailed t-test). **(c)** Amperometric measurement of extracellular LL tone in organotypic brainstem slices transduced with AVV-PRSx8EGFP alone (Control, n=14) or in combination with AVV-sGFAP-LOX-IRES-tdTomato (LOX, n=12; Mann–Whitney U rank test). **(d)** Representative traces of Laconic FRET ratio in dissociated astrocytic cultures expressing AVV-CMV-Laconic alone (Control) or in combination with AVV-sGFAP-LOX-IRES-tdTomato and exposed to pyruvate (10mM; highlighted application time). **(e)** Minimum Laconic FRET ratios in control and LOX-expressing astrocytes evoked by extrusion of intracellular LL via transacceleration of MCTs (n=62 cells in Control; n=52 cells in LOX; unpaired two-tailed t-test). **(f)** Representative trace of an amperometric recording in organotypic brainstem slices during pyruvate-induced transacceleration. **(g)** Trans-acceleration and **(h)** depletion amplitude, respectively, following

pyruvate (10mM) exposure in slices transduced with AVV-PRSx8EGFP alone (Control, n=11) or in combination with AVV-sGFAP-LOX-IRES-tdTomato (LOX, n=12); unpaired two-tailed t-test **(g)** or Mann–Whitney U rank test **(h)**.

Figure 3. Expression of LOX in hippocampal astrocytes leads to novelty-induced activity. **(a)** Serial coronal sections of the mouse brain with control vector (LVV-sGFAP-IRES-tdTomato) injection in the hippocampus and stained with anti-RFP (green); scale bars 500 µm. **(b)** Representative images of hippocampal sections with tdTomato$^+$ astrocytes (red) co-stained with anti-RFP (green); scale bars – 50µm. **(c)** In the holeboard test mice expressing LOX in hippocampal astrocytes manifested increased activity compared to control LVV injected mice; **(d)** During habituation to the trace fear conditioning chamber, mice expressing LOX in hippocampal astrocytes showed less freezing in response to a novel environment; *p<0.05, n=8-9. **(e)** Hippocampal LVV-sGFAP-LOX-IRES-tdTomato injections improved the performance in the task for spatial recognition memory in the Y maze task **(a)**, with no change in the y-maze spontaneous alternation task **(f)** or the novel object recognition test **(g)**; **p<0.01, n=5-9.

Figure 4. Viral vector mediated expression of LOX in astrocytes as a novel tool for accelerated breakdown of intracellular LL. Constitutive activity of LOX breaks down LL produced through glycolysis in astrocytes and, consequently, decreases intra-astrocytic LL concentration and subsequent release to the extracellular space. This has implications for constitutive as well as stimulus-evoked LL release and for metabolic and signalling roles of LL in the brain.

Supplemental Figure Legends

Suppl Figure 1. Cassette for expression of LOX in cell lines and in astrocytes *in vitro* and *in vivo*. (a) LOX and control constructs in plasmids for CMV-driven expression in acutely transfected HEK293 cells – *CMV-LOX-IRES-EGFP* and *CMV-IRES-EGFP*, respectively. Enhanced green fluorescent protein (EGFP) serves as expression marker and is preceded by an internal ribosomal entry site (IRES). **(b)** Construct in adenoviral vector (AVV) backbone for expression of LOX and fluorescent marker in astrocytes *in vitro* – *AVV-sGFAP-LOX-IRES-tdTomato*. A transcriptionally enhanced short glial fibrillary acidic protein promoter (sGFAP; Liu et al., 2008) restricts expression to astrocytes. tdTomato was used as fluorescent marker. **(c)** Cassettes in lentiviral vector (LVV) backbone for expression of LOX and control fluorescent marker in astrocytes *in vivo* (Duale et al., 2005) – *LVV-sGFAP-LOX-IRES-tdTomato* and *LVV-sGFAP-IRES-tdTomato*, respectively. A Woodchuck Hepatitis Virus posttranscriptional regulatory element (WPRE) was included to stabilise expression levels.

Suppl Figure 2. Representative images of co-expression of fluorescent reporters with LOX *in vitro*. (a) EGFP expression in CMV-LOX-IRES-EGFP transfected HEK293 cells. **(b)** Dissociated cultures of rat astrocytes transduced with AVV-sGFAP-LOX-IRES-tdTomato. **(c)** Organotypic brainstem slice cultures transduced with AVV-sGFAP-LOX-IRES-tdTomato. tdTomato signal amplified by anti-RFP staining in (b) and (c). Scale bars 50 µm.

Suppl Figure 3. Astrocyte specific expression in hippocampus *in vivo* following transduction with LVV-sGFAP-LOX-IRES-tdTomato. (a) Representative images of tdTomato$^+$ (red) astrocytes co-stained with anti-S100β (green) antibody. **(b)** Representative images of tdTomato$^+$ (red) astrocytes co-stained with anti-GFAP (green) antibody. Scale bars 10 µm.

Suppl Figure 4. Lack of neuronal and microglial expression *in vivo* following transduction with LVV-sGFAP-LOX-IRES-tdTomato. Representative images of tdTomato$^+$ (red) astrocytes co-stained with anti-IBA1 (green) or anti-NeuN (magenta) antibody. Scale bar 10µm.

Suppl Figure 5. No effects of LOX expression in hippocampal astrocytes on locomotor activity. Locomotor activity was measured during 30 minutes in the open field. Total activity **(a)**, total rearing **(b)**, central **(c)** and peripheral **(d)** locomotor activities were not different between animals expressing LOX and controls; $p>0.05$, n=8-9.

Suppl Figure 6. No effects of LOX expression in hippocampal astrocytes on anxiety-related or exploratory behaviours. Anxiety-like behaviors were evaluated in the elevated plus maze (EPM). There was no difference in percent of time spent in the open arms **(a)** and the distance travelled **(b)** between control and LOX groups. **(c)** Exploratory behavior was examined in in the holeboard test. There was no significant difference in the number of head dips between control and LOX groups. $p > 0.05$, n=8-9.

Suppl Figure 7. No effects of LOX expression in hippocampal astrocytes on trace fear conditioning. (a) No difference in freezing behaviour was found between control and LOX groups during the training session, where a 20 sec tone, followed by a 2 sec shock, was delivered four times as indicated. No difference was observed 24 hours after the training session in context-dependent memory **(b)**, nor in cue-dependent memory **(c)**; p 0.05, n=8-9.

Figure 1.

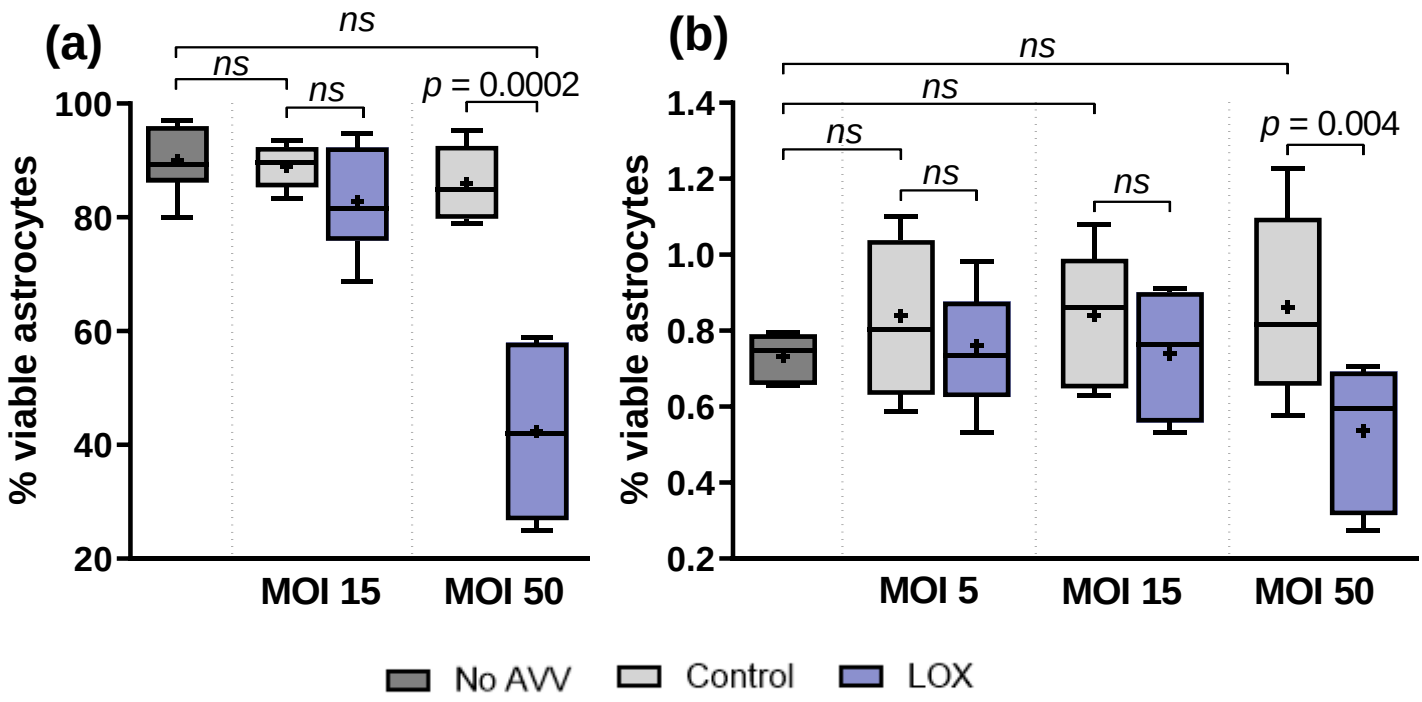
(a)
ns
ns
ns
p = 0.0002
100
80
60
40
20
% viable astrocytes
MOI 15
MOI 50
(b)
ns
ns
ns
ns
p = 0.004
1.4
1.2
1.0
0.8
0.6
0.4
0.2
% viable astrocytes
MOI 5
MOI 15
MOI 50
No AVV
Control
LOX

Figure 2.

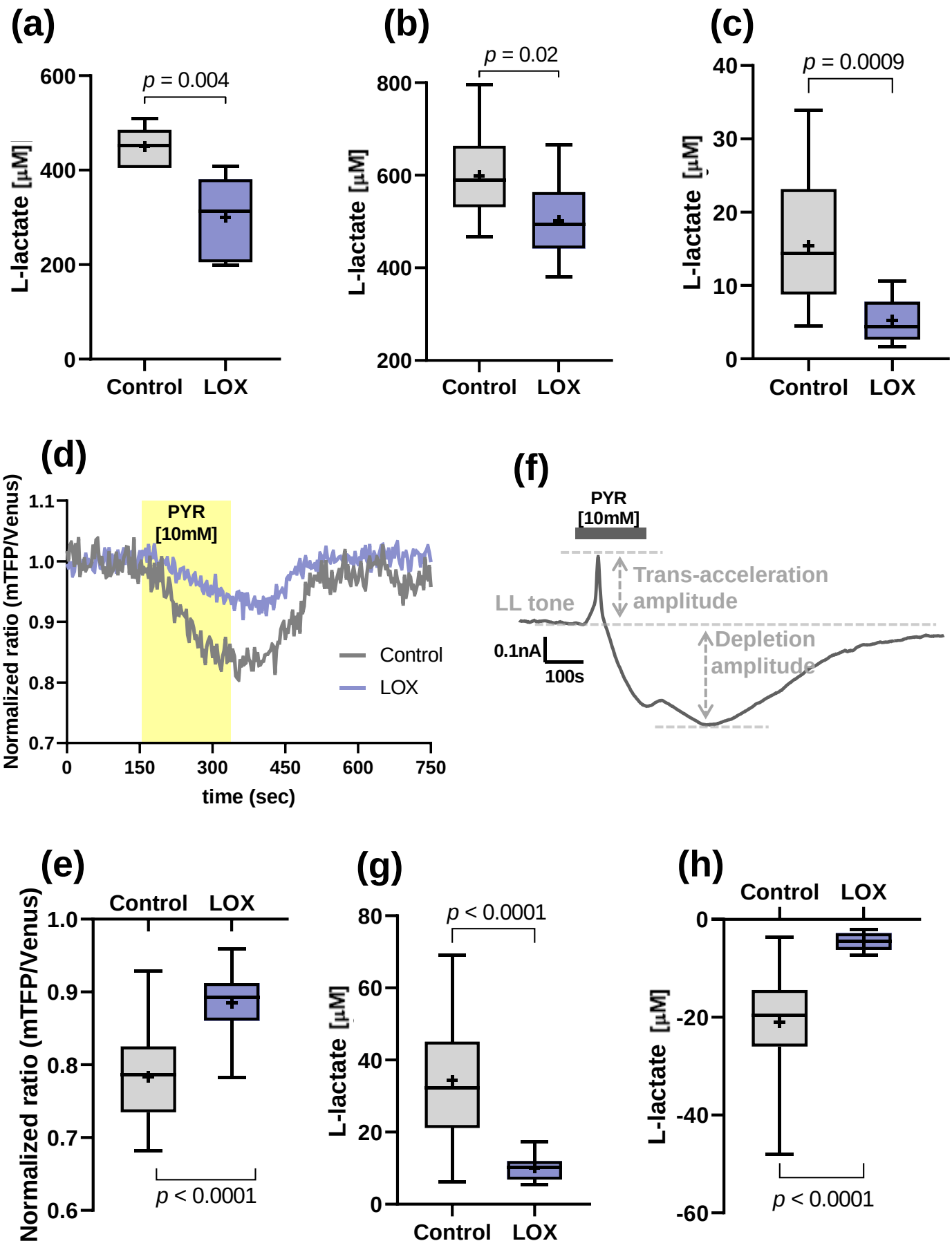
(a)
p = 0.004
L-lactate [μM]
600
400
200
0
Control
LOX
(b)
p = 0.02
L-lactate [μM]
800
600
400
200
Control
LOX
(c)
p = 0.0009
L-lactate [μM]
40
30
20
10
0
Control
LOX
(d)
PYR
[10mM]
Normalized ratio (mTFP/Venus)
1.1
1.0
0.9
0.8
0.7
0
150
300
450
600
750
time (sec)
Control
LOX
(f)
PYR
[10mM]
LL tone
Trans-acceleration
amplitude
Depletion
amplitude
0.1nA
100s
(e)
Control
LOX
Normalized ratio (mTFP/Venus)
1.0
0.9
0.8
0.7
0.6
p < 0.0001
(g)
p < 0.0001
L-lactate [μM]
80
60
40
20
0
Control
LOX
(h)
Control
LOX
L-lactate [μM]
0
-20
-40
-60
p < 0.0001

Figure 3.

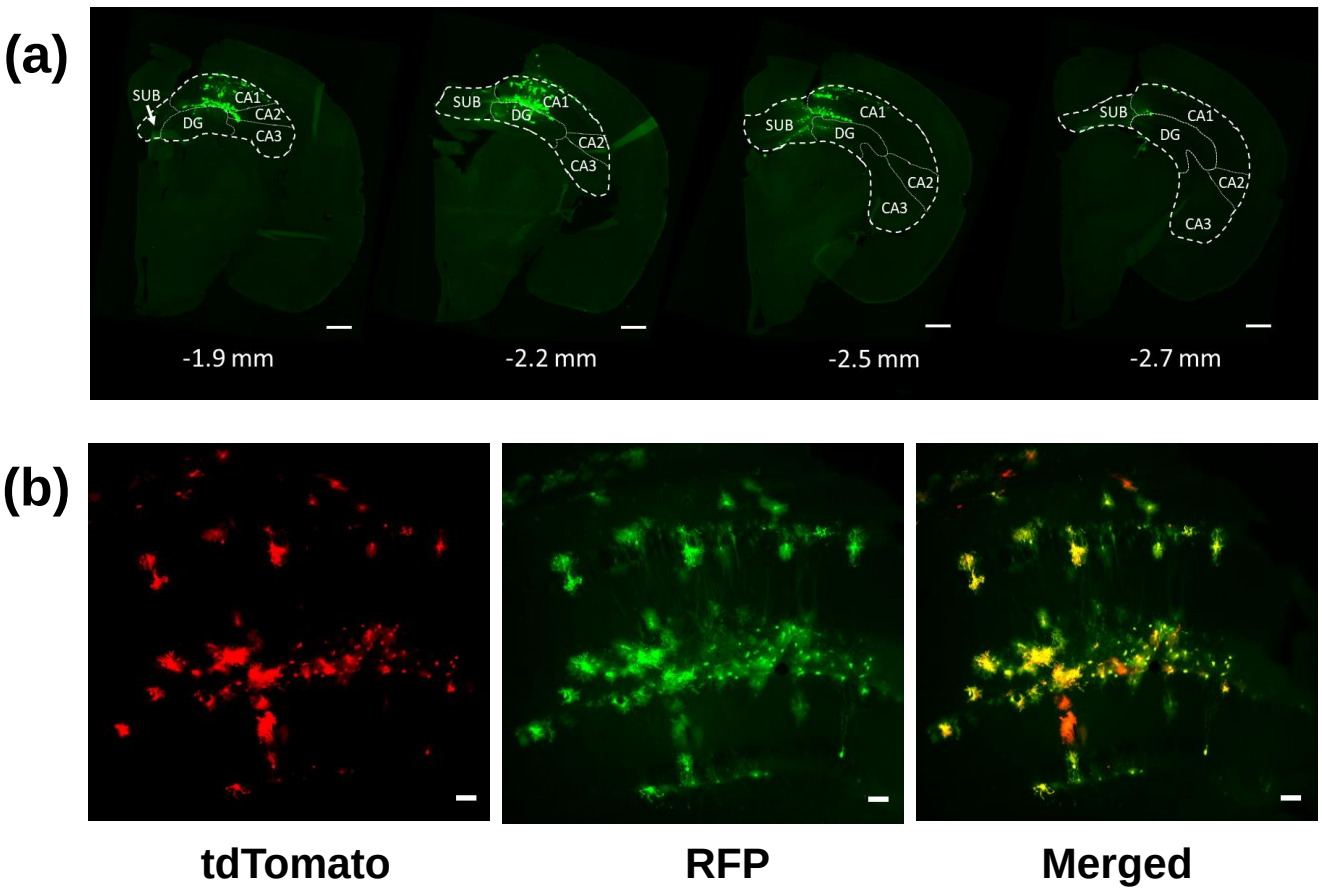
(a)
SUB
CA1
DG
CA2
CA3
-1.9 mm
-2.2 mm
-2.5 mm
-2.7 mm
(b)
tdTomato
RFP
Merged
(c)
p = 0.04
Distance (m)
Control
LOX
(d)
% Freezing
Time (minutes)
Control
LOX
p = 0.004
(e)
p = 0.009
% Time in Novel Arm
Control
LOX
(f)
% Alternation
Control
LOX
(g)
% Time
Familiar Object
Novel Object
Control
LOX

Figure 4.

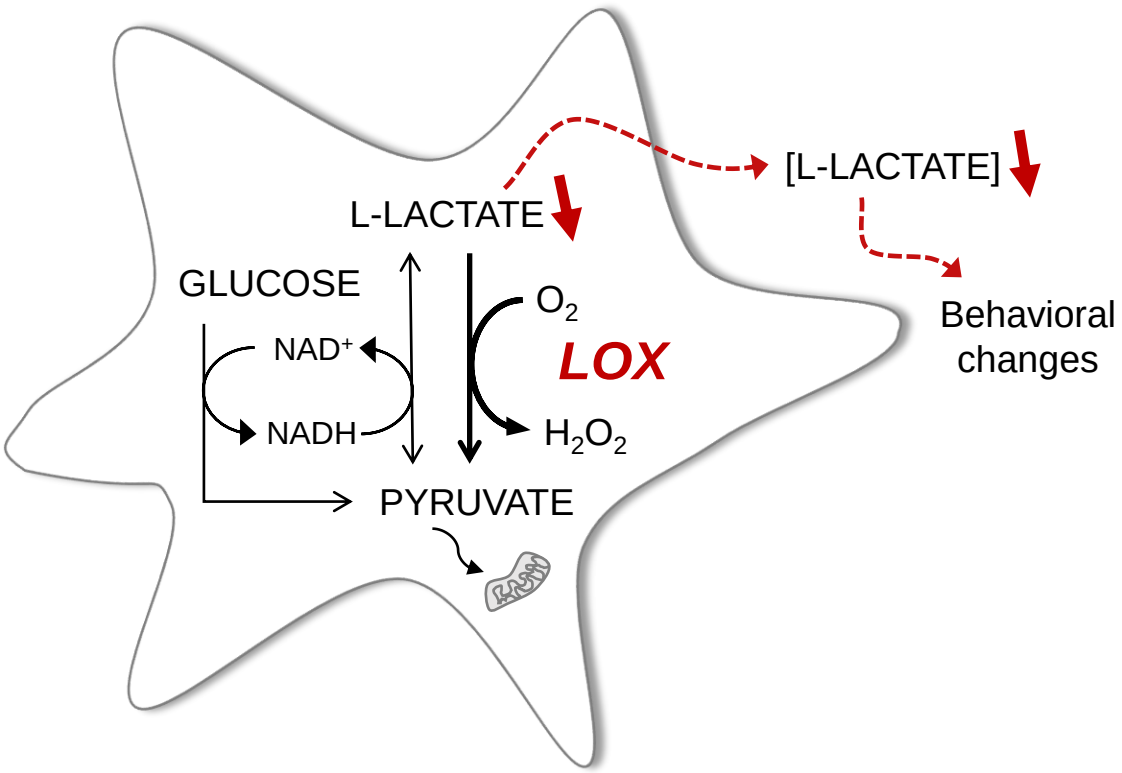
[L-LACTATE]
L-LACTATE
GLUCOSE
O2
LOX
NAD+
NADH
H2O2
PYRUVATE
Behavioral changes

Suppl Table 1. Antibody information

Primary Antibody for Immunohistochemistry	Species	Dilution	Source	Cat #
Anti-Glial Fibrillary Acidic Protein (GFAP) chicken polyclonal antibody mixture	chicken	1:1000	Aveslab	GFAP
Anti-Iba1 Antibody	rabbit	1:1000	Wako Chemicals	019-19741
Anti-NeuN Antibody	guinea pig	1:1000	Synaptic Systems	266 004
Anti- RFP Antibody Pre-adsorbed	rabbit	1:1000 1:200	Rockland Immunochemicals, Inc.	600-401-379S
Anti-S100 beta Antibody	rabbit	1:1000	Abcam	EP1576Y
Secondary Antibody for Immunohistochemistry	**Species**	**Dilution**	**Source**	**Cat #**
Goat anti-Rabbit IgG (H+L) Cross-Adsorbed ReadyProbes™ Secondary Antibody, Alexa Fluor 594	goat	n/a	Thermo Fisher Scientific	R37117
Goat anti-Guinea Pig IgG (H+L) Highly Cross-Adsorbed Secondary Antibody, Alexa Fluor 633	goat	1:1000	Thermo Fisher Scientific	A-21105
Goat anti-Rabbit IgG (H+L) Highly Cross-Adsorbed Secondary Antibody, Alexa Fluor 488	goat	1:1000	Thermo Fisher Scientific	A-11075
Goat anti-Chicken IgY (H+L) Secondary Antibody, Alexa Fluor 488	goat	1:1000	Thermo Fisher Scientific	A-11039

Suppl Figure 1.

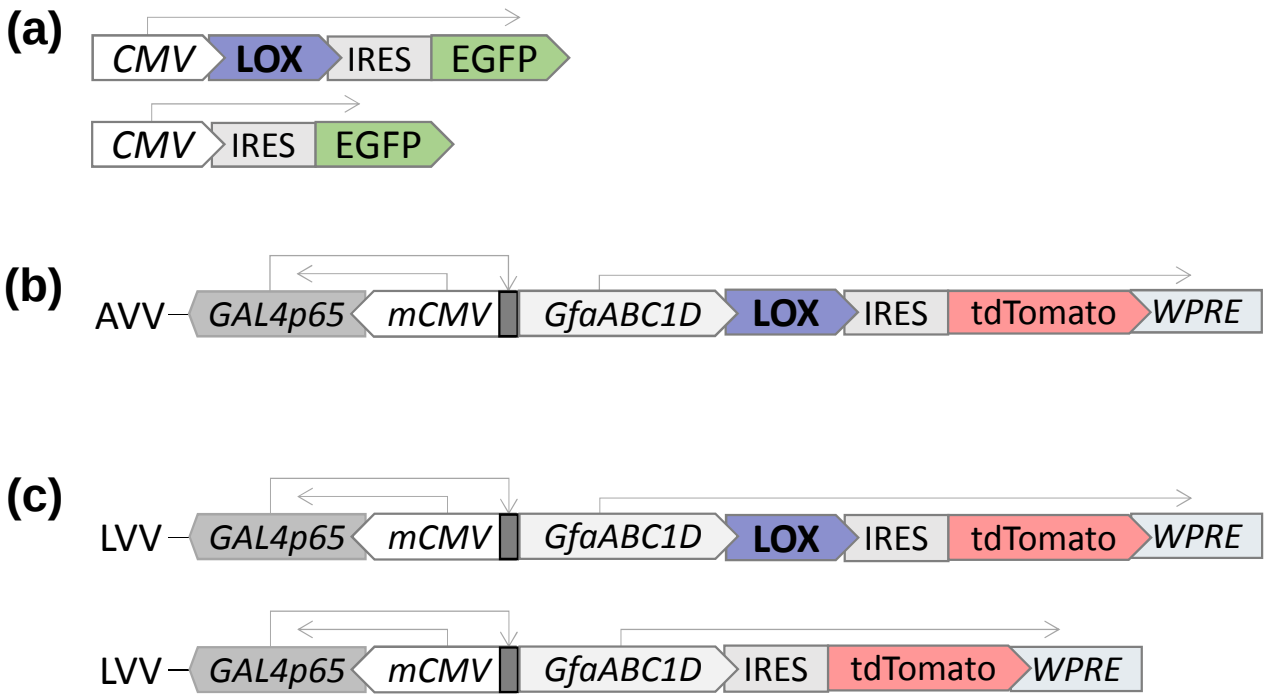

Suppl Figure 2.

(a)

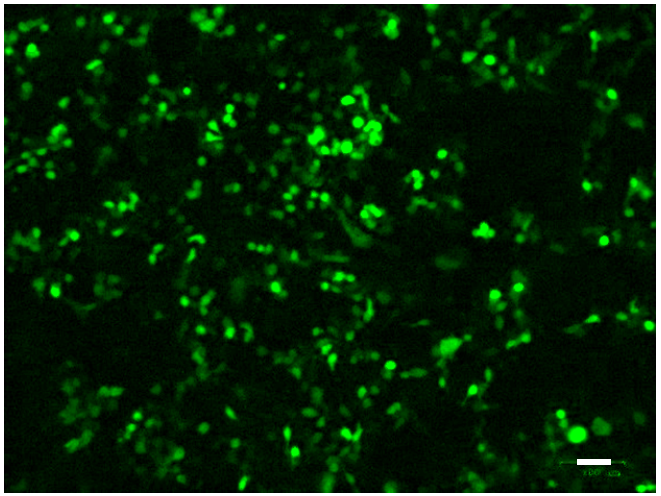

(b)

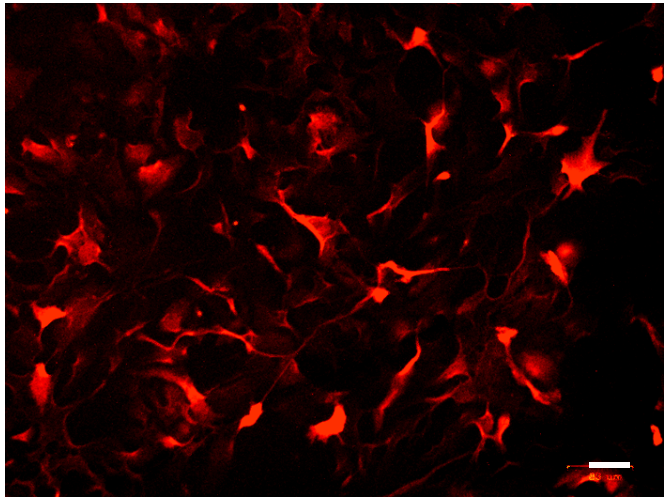

(c)

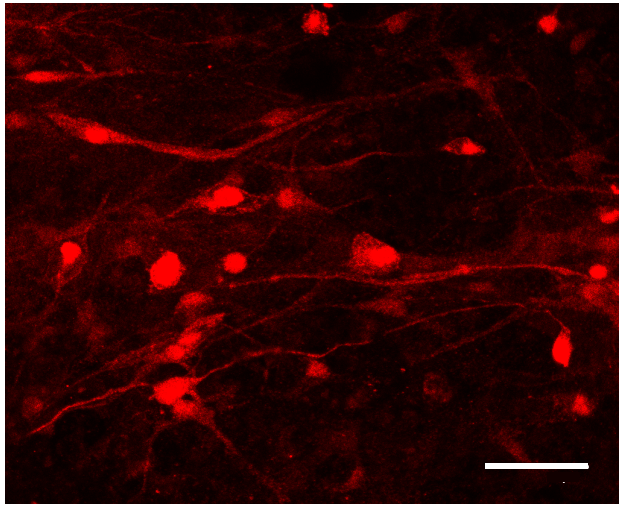

Suppl Figure 3.

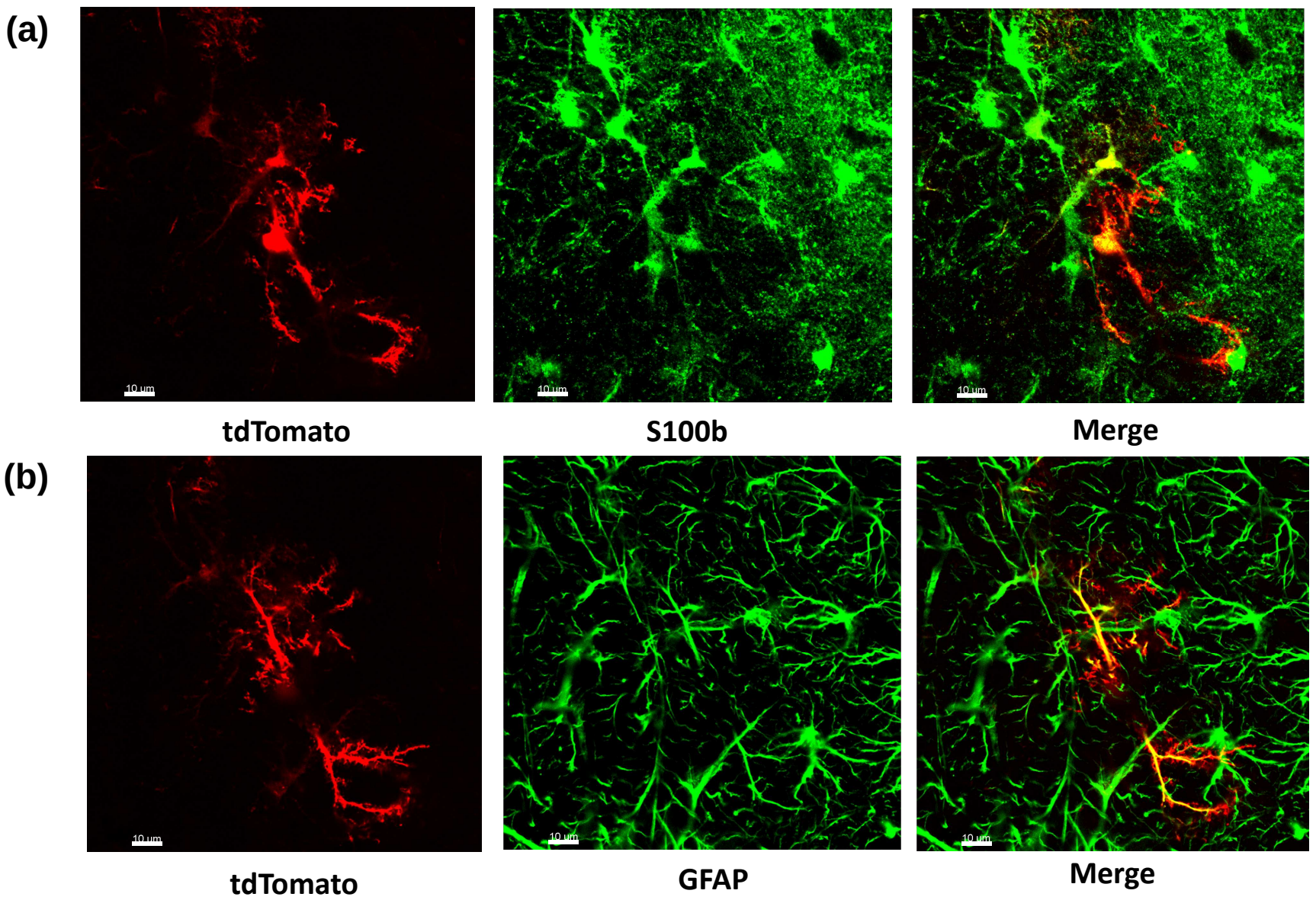

Suppl Figure 4.

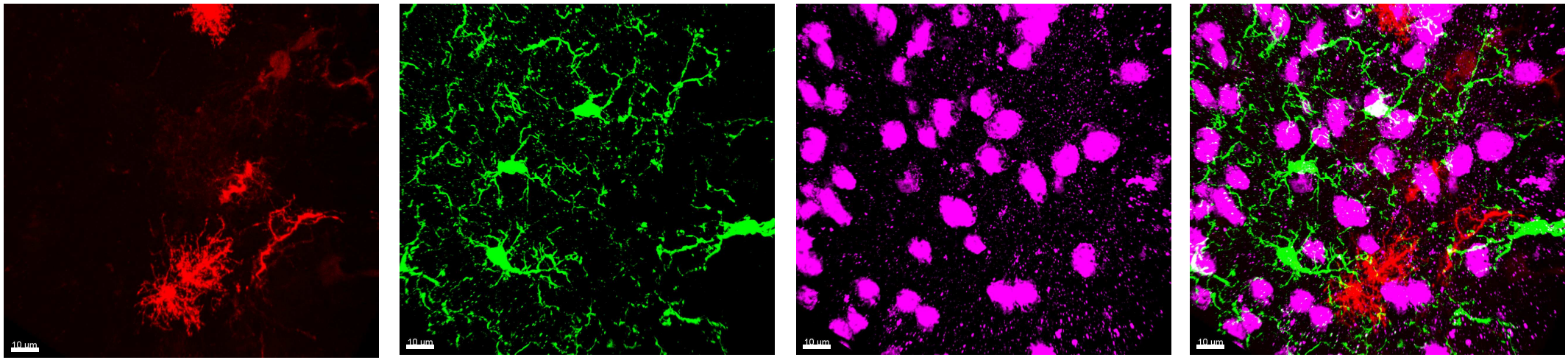

tdTomato IBA1 NeuN Merge

Suppl Figure 5.

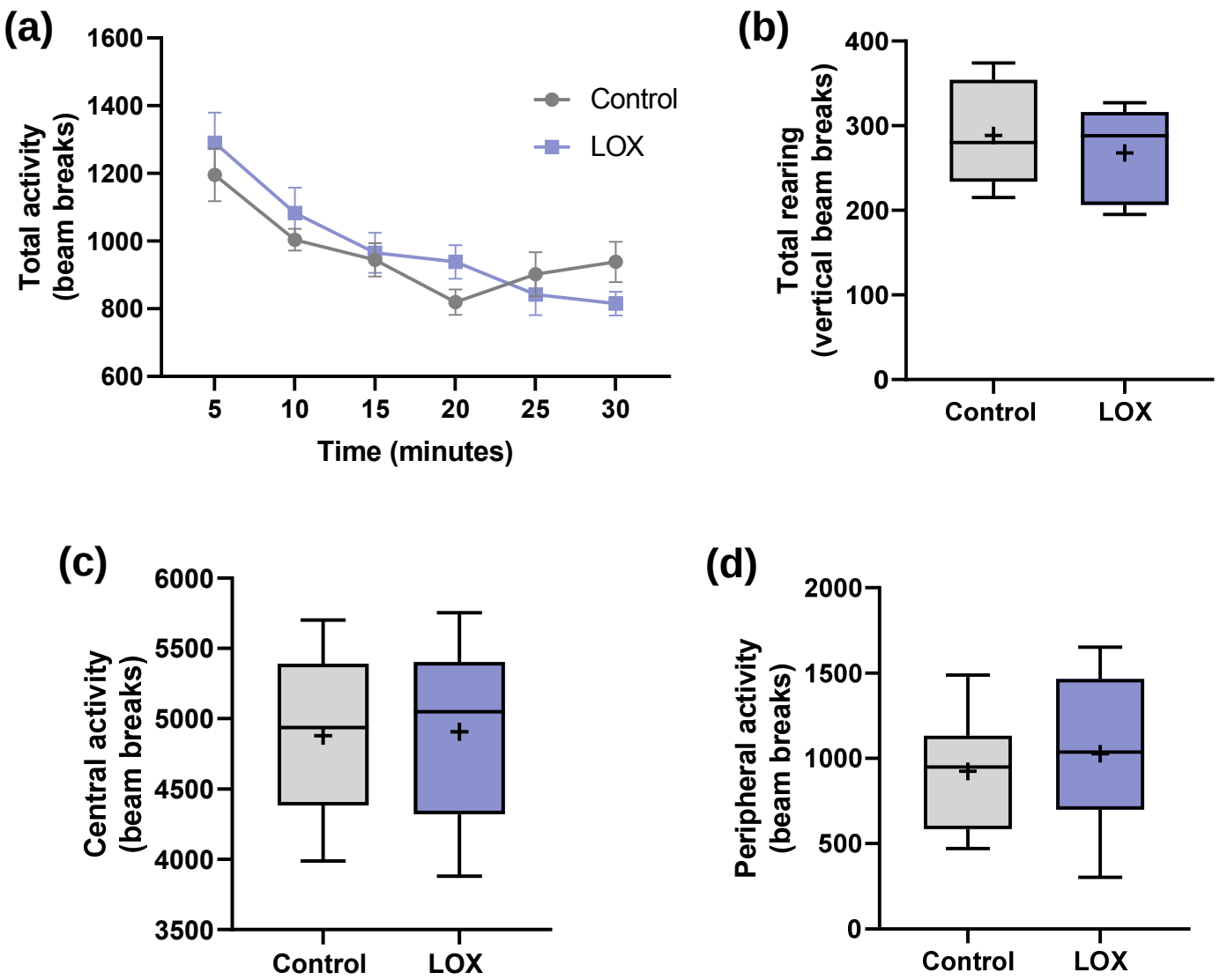

Suppl Figure 6.

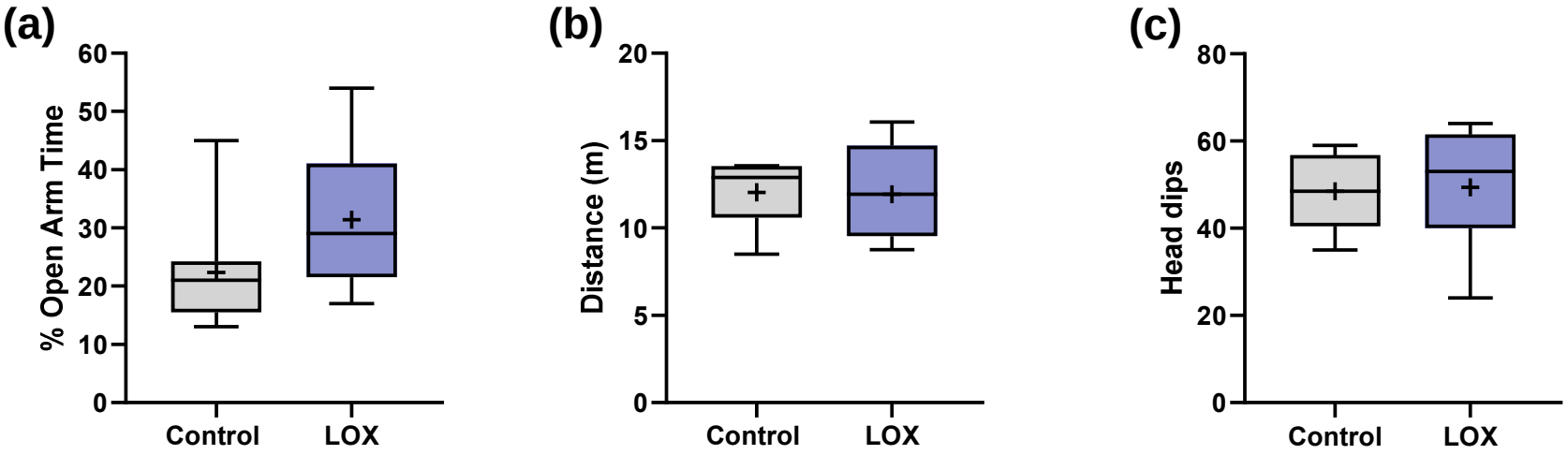

Suppl Figure 7.